ISCI, Volume *17*

Supplemental Information

Nanoengineered Metasurface Immunosensor with over 1000-Fold Electrochemiluminescence Enhancement for Ultra-sensitive Bioassay

Chuanping Li, Shanshan Wang, Haijuan Li, Muhammad Saqib, Chen Xu, and Yongdong Jin

Supplemental Information

Core/Shell/Gap-Nanoengineered Metasurface Immunosensor with over 1000-Fold Electrochemiluminescence Enhancement for Ultra-sensitive Bioassay

Chuanping Li[1,2,4,5], Shanshan Wang[1,3,5], Haijuan Li[1], Muhammad Saqib[1], Chen Xu[1] & Yongdong Jin[1,2,*]

[1]State Key Laboratory of Electroanalytical Chemistry, Changchun Institute of Applied Chemistry, Chinese Academy of Sciences, 5625 Renmin Street, Changchun 130022, P. R. China.

[2] University of Chinese Academy of Sciences, Beijing 100049, P. R. China.

[3] College of Chemistry, Liaoning University, Shenyang 110036, P. R. China.

[4] current address: College of Biological and Chemical Engineering, Anhui Polytechnic University, Wuhu 241000, P. R. China.

[5] These authors contributed equal to this work.

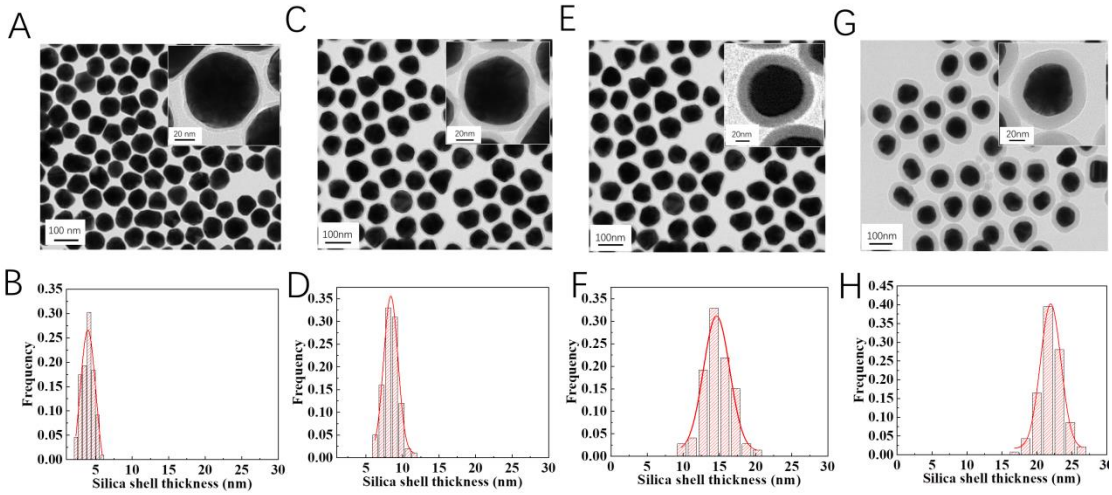

Figure S1. TEM images and silica shell thicknesses distributions of 75 nm Au@SiO_2 NPs. (A-B) 75 nm Au@4.0 ± 0.8 nm SiO_2 NPs, (C-D) 75 nm Au@8.4 ± 1.1 nm SiO_2 NPs, (E-F) 75 nm Au@14.9 ± 2.0 nm SiO_2 NPs, (G-H) 75 nm Au@24.6 ± 2.7 nm SiO_2 NPs. Data are represented as mean $\pm$ TEM. Related to Figure 2.

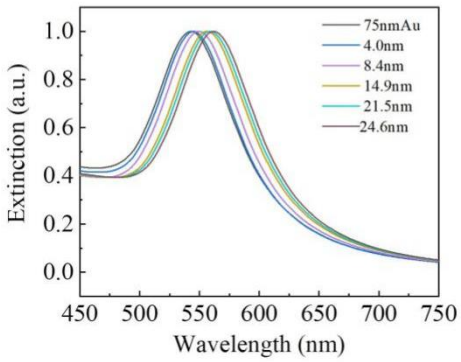

Figure S2. UV-Vis spectra of the 75 nm Au@SiO_2 NPs. Related to Figure 2.

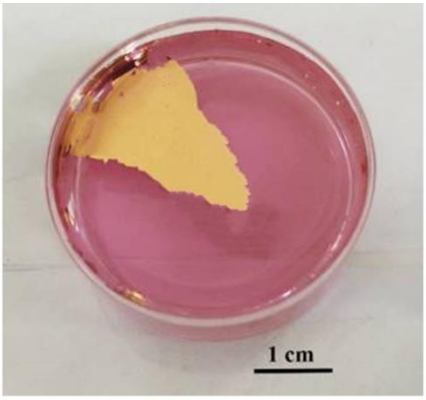

Figure S3. Photograph of the monolayered 75 nm Au@21.5 nm SiO_2 nanomembrane. Related to Figure 2.

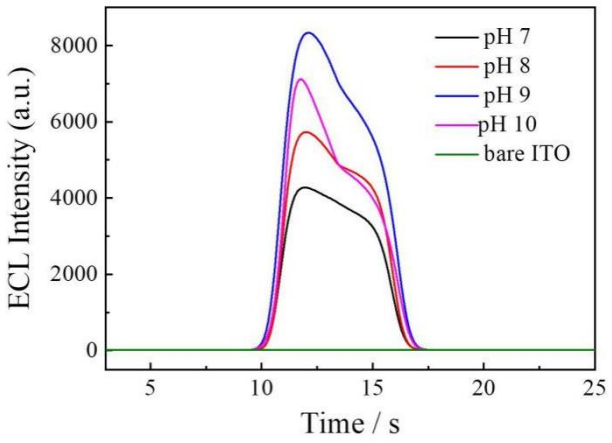

Figure S4. ECL intensity of the 75 nm Au@21.5 nm SiO_2 modified MASNE at 0.1 M PBS solution (containing 20 μM $Ru(bpy)_3^{2+}$ and 0.1 mM tri-n-propylamine (TPrA)) with different pH value. Related to Figure 3.

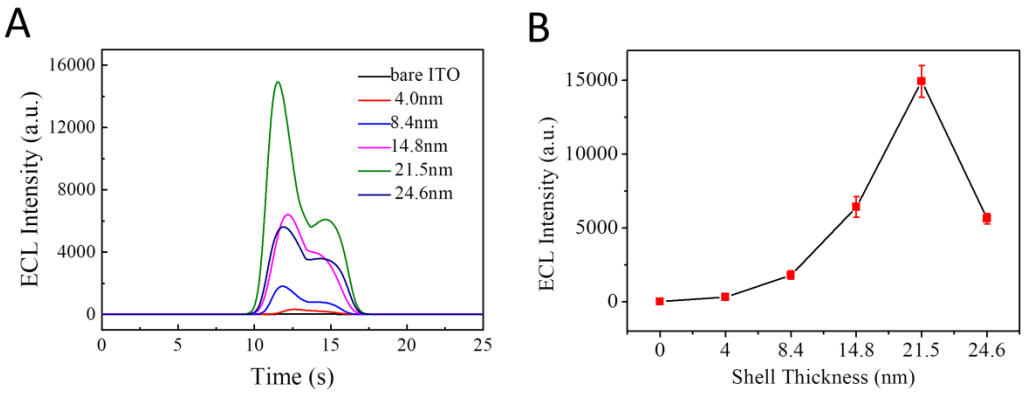

Figure S5. ECL intensity of the 75 nm Au@ SiO_2 modified MASNE with different silica shell thicknesses (0.1 M PBS solution (pH=9) containing 20 μmol L^{-1} $Ru(bpy)_3^{2+}$ and 0.1 mmol L^{-1} TPrA). Related to Figure 3.

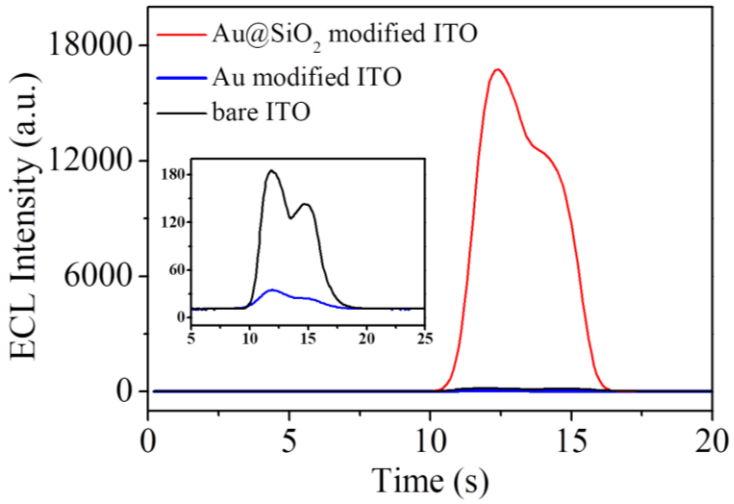

Figure S6. The comparison of ECL intensity between 75nm Au@21.5 nm SiO_2 NPs and 75 nm AuNPs fabricated ECL electrodes using Ru@SiO_2 as luminophore. Inset: enlarged image of ECL intensity of Au modified ITO and bare ITO electrode. Related to Figure 3.

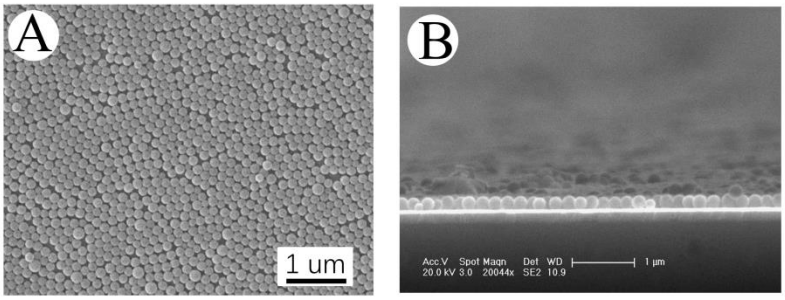

Figure S7. SEM images of the fabricated monolayered SiO_2 nanomembrane-based ECL electrode. (A) Top view, (B) Side view of the SEM image. Related to Figure 3.

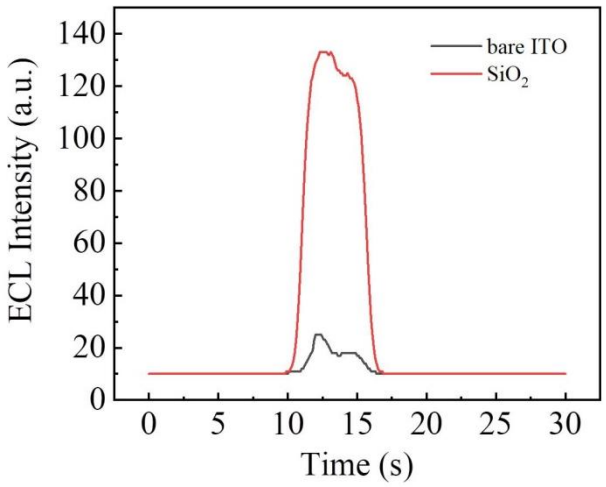

Figure S8. ECL intensity of bare SiO_2NPs fabricated MASNE in 0.1 M PBS (pH=9) buffer containing 20 µ M $Ru(bpy)_3^{2+}$ and 0.1 mM tripropylamine (TPrA). Related to Figure 3.

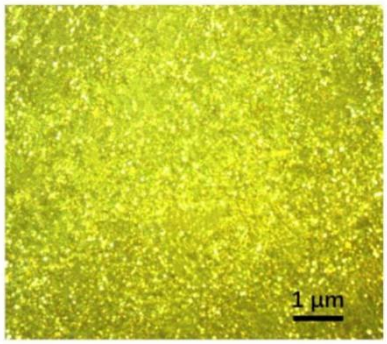

Figure S9. Microscopy-based selected area dark field scattering image of the MASNE constructed with 75 nm Au@21.5 nm SiO_2 NPs. Related to Figure 3.

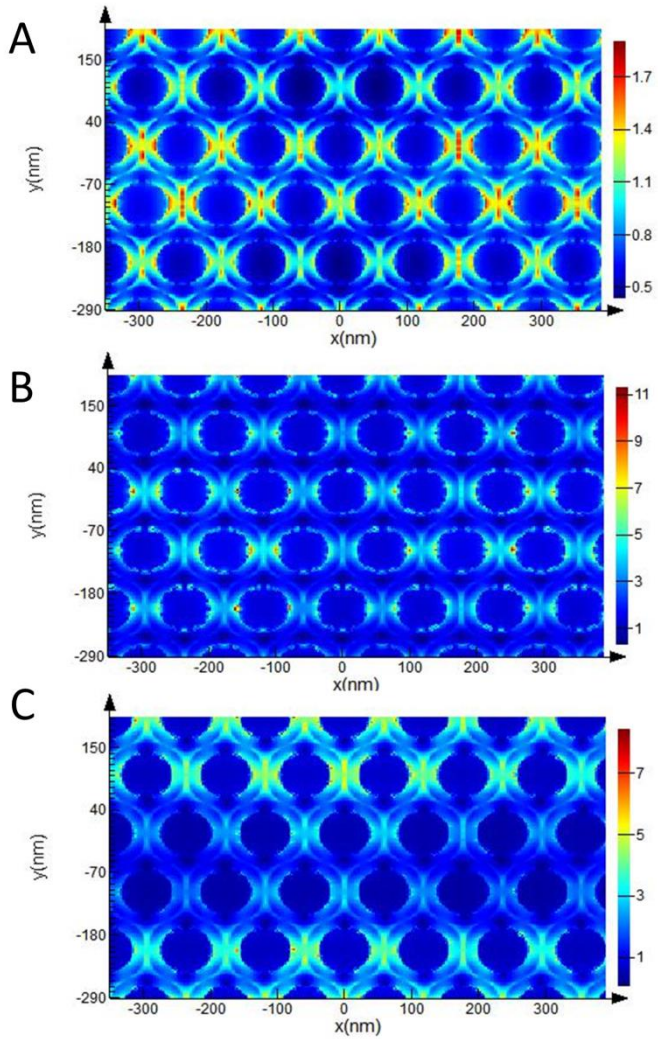

Figure S10. Wavelength dependent EM field enhancement with excitation light of (A) 450 nm, (b) 550 nm, (c)700 nm**.** Related to Figure 3.

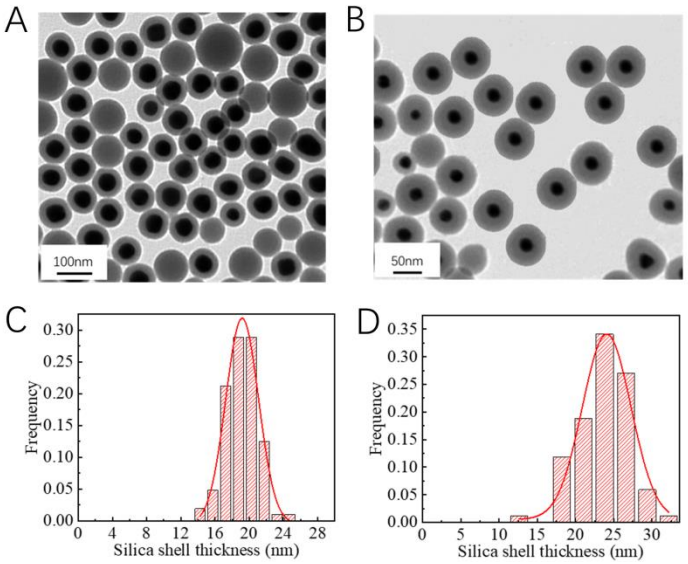

Figure S11. TEM images and silica shell thicknesses distributions of Au@SiO_2 NPs. (A, C) 50 nm Au@19.9±1.9 nm SiO_2. (B, D) 20 nm Au@22.5±3.2 nm SiO_2. Related to Figure 3.

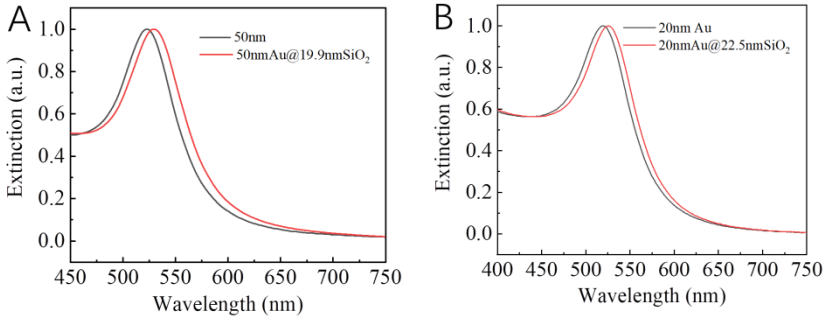

Figure S12. UV-Vis spectra of Au@SiO_2 NPs. (A) 50 nm Au@19.9±1.9 nm SiO_2. (B) 20 nm Au@22.5±3.2 nm SiO_2. Related to Figure 3.

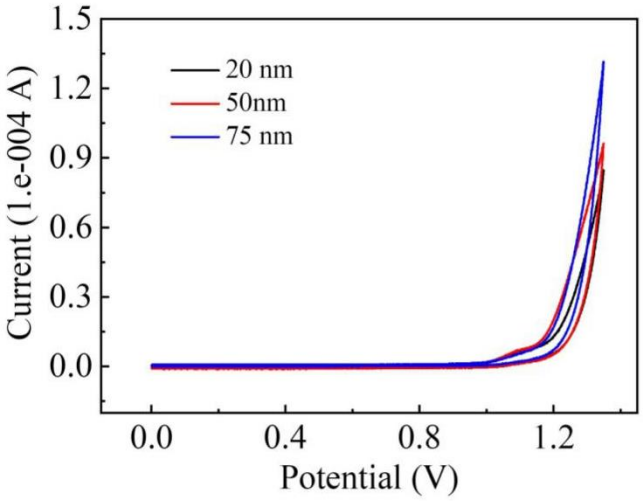

Figure S13. Simultaneous electrochemical measurements of ECL electrodes modified with different Au@21.5 nm SiO_2 NPs. Related to Figure 3.

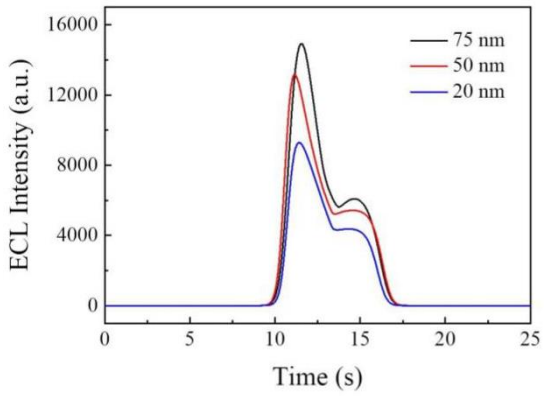

Figure S14. The ECL intensity of the Au@21.5 nm SiO_2-based MASNEs with different AuNPs sizes in 0.1 M PBS (pH=9) buffer containing 20 μM $Ru(bpy)_3^{2+}$ and 0.1 mM tripropylamine (TPrA). Related to Figure 3.

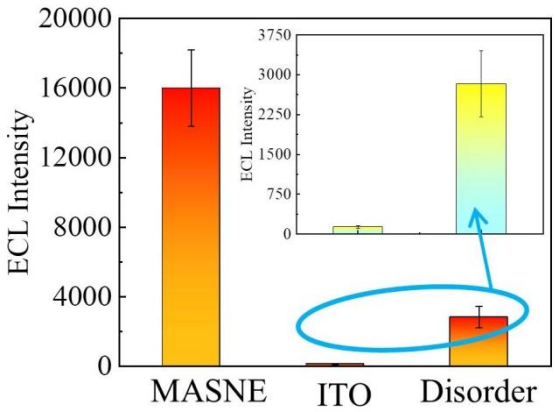

Figure S15. Comparation of ECL intensity between 75 nm Au@21.5 nm SiO_2 NPs-based MASNE, ITO and disorderly stacked 75 nm Au@21.5 nm SiO_2 NPs fabricated ECL electrode. Related to Figure 3.

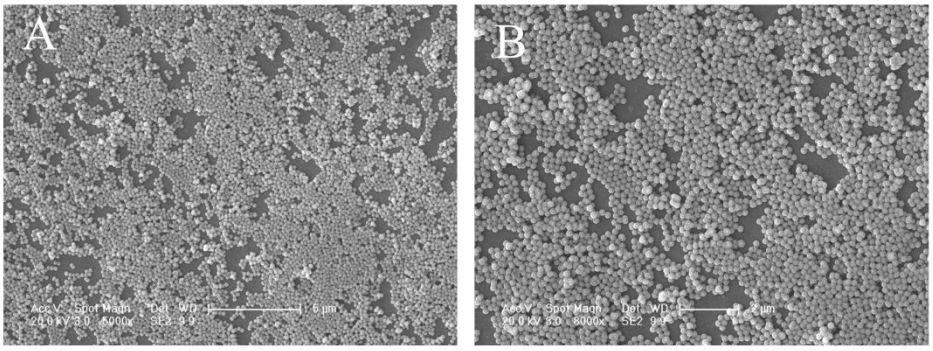

Figure S16. SEM images of the disordered Au@SiO_2 fabricated ECL electrode. Related to Figure 3.

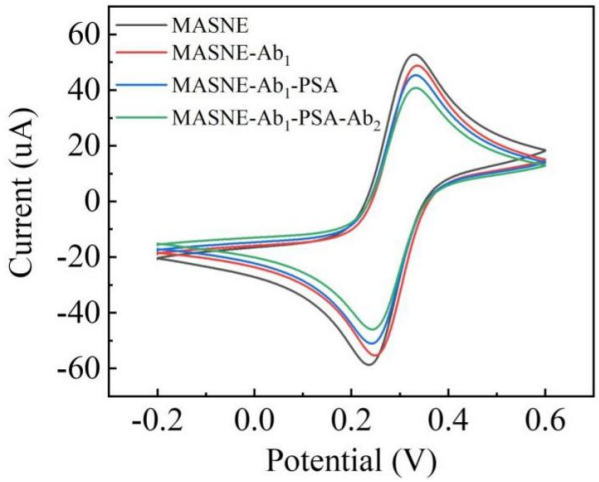

Figure S17. Cyclic voltammograms (in 2 mM $K_3Fe(CN)_6$ solution, sweep rate 50 mV/s) for the ECL sensing platform during the fabrication. Compared with the bare MASNE, the peak current decreases after every modification step because of the poor conductivity of the biomolecules and Ru@SiO_2. Related to Figure 5.

Table S1. Comparison of ECL immunosensor with other reported immunosensors for determination of PSA. Related to Figure 5.

methods	linear range	detection limit	reference
electrochemical	-	0.9 pg mL^{-1}	(Zheng et al., 2005)
enzyme-linked immunosorbent assay	-	14 fg mL^{-1} (0.4 fM)	(Rissin et al., 2010)
electrochemical	0.4-40 ng mL^{-1}	4 pg ml^{-1}	(Yu et al., 2006)
SERS	5.0 pg mL^{-1}-50 ng mL^{-1}	0.012 ng mL^{-1}	(Cheng et al., 2017)
Bio-bar-code assay	-	0.003-0.03 fM	(Nam et al., 2003)
ECL	0.5-500 ng mL^{-1}	0.058 ng mL^{-1}	(Shao et al., 2018)
ECL	5.0 pg mL^{-1}-5.0 ng mL^{-1}	0.8 pg mL^{-1}	(Qi et al., 2014)
ECL	10 fg mL^{-1}-1 μg mL^{-1}	3 fg mL^{-1}(~0.1 fM)	This work

Transparent Methods

Materials

3-Aminopropyltrimethoxysilane (APTMS), Tri(2,2'-bipyridyl)dichlororuthenium (Ⅱ) hexahydrate ($Ru(bpy)_3Cl_2,6H_2O$), Sodium citrate (Na_3CA), Tripropylamine (TPrA), sodium silicate (Na_2SiO_3) were purchased from Sigma-Aldrich. $HAuCl_4·4H_2O$, methanol, n-hexane were purchased from Beijing Chemical Factory (Beijing, China). Tetraethyl orthosilicate (TEOS) and Triton X-100 (TX-100) were purchased from Aladdin Co., Ltd. ITO-coated glass was purchased from Zhuhai Kaivo Optoelectric Technology Co., Ltd. 3-(Triethoxysilyl)propylsuccinic anhydride was purchased from Innochem Co., Ltd. Bovine serum albumin (BSA), IgG, Mb, PSA, AFP, cTnI were purchased from Sinopharm Chemical Reagent Co. Ltd. (Beijing, China). All of the chemicals were used without further purification. Water used throughout all these experiments was purified with a Millipore system (18.2 MΩ· cm).

Characterization

The size and morphologies of the $Au@SiO_2$ NPs were characterized with a JEM-2100F transmission electron microscope (TEM) and scanning electron microscope (SEM) images were performed with an XL30 ESEM SEM. The UV−vis absorption spectra were obtained by a UV-2600 spectrophotometer (Shimadzu). Optical microscopy-based selected area dark-field scattering images and spectra were obtained by using an inverted Leica DMI6000B microscope (Germany), equipped with a Princeton spectrometer (PIXIS 256). The ECL experiments were performed on a MPI-A multifunctional electrochemical and chemiluminescent analytical system (Xi'An Remax Electronic Science & Technology Co. Ltd., 350-650 nm). The voltage of the photomultiplier tube (PMT) was set at 500 V. The experiments were carried out with a conventional three-electrode system. The working, counter and reference electrodes were ITO electrode, Pt wire and Ag/AgCl electrode, respectively.

Synthesis of $Au@SiO_2$ NPs

The AuNPs with different size were synthesized by the methods reported elsewhere.(Frens, 1973; Haiss et al., 2007) $Au@SiO_2$ NPs of different silica shell

thicknesses were synthesized by the method reported by Tian's group and our previous work (Li et al., 2010) with minor modification. Typically, 700 μL of fresh prepared 1 mM APTMS was drop-wise added to 30 mL of 75 nm gold sol and stirred for 20 min vigorously; then about 4 mL of 0.54% Na_2SiO_3 and 100 μL of 0.1 M H_2SO_4 was added in the mixture and heated at 90 ℃ for a period of time. After cooling to the room temperature, the nanoparticles were centrifuged at 4000 rpm for 18 min and diluted to 10 mL with deionized water. Au@SiO_2 NPs with tunable shell-thickness (4~8 nm) can be obtained by carefully controlling the reaction time, pH and concentration. In order to further increase the silica shell thickness, 10 mL Au@8 nm SiO_2NPs obtained were added to a mixture of 40 mL ethyl alcohol and 600 μL NH_3 H_2O, then a certain amount of 1% TEOS were added. After stirring at room temperature for 12, 24, 36 h, Au@SiO_2 NPs with silica shell thicknesses of ~15, ~22 and ~25 nm were obtained respectively.

Modification of Au@SiO_2 NPs

In order to improve the quality of the self-assembled nanomembrane, Au@SiO_2 NPs with silica shell thicknesses of ~15 nm, ~22 nm, ~25 nm were carboxylated with 3-(Triethoxysilyl)propylsuccinic anhydride by the following steps. Firstly, the as-prepared Au@SiO_2 NPs were centrifuged at 5000 rpm three times and diluted with isopropanol. Then, 0.5 mL of 10 mM 3-(Triethoxysilyl)propylsuccinic anhydride were added and heated at 85℃ for 24 h. Finally, the nanoparticles were centrifuged at 6000 rpm for three times and diluted with deionized water to 10 mL.

Fabrication of monolayered Au@SiO_2 nanomembrane-based ECL electrode (MASNE)

ITO glass was firstly cleaned with sonication in water, acetone, ethyl alcohol and finally in water for 10 min, respectively. Then, each slide was placed in a solution of 5:1:1 H_2O + 30% H_2O_2+25% NH_3 and heated at 80 ℃ for about 20 min. Finally, the ITO glasses were dried with N_2. The monolayer Au@SiO_2 nanomembranes were prepared by a method of liquid/liquid interface self-assembly (LLISA). Typically, 3 mL of Au@SiO_2 NPs was added to a plastic container, then 460 μL of n-hexane was added to form a two-phase interface. Then, 3.7 mL of methanol was poured rapidly

into the mixture to capture the nanoparticles at the hexane/water interface. After the evaporation of hexane, the nanoparticles were simultaneously self-assembled into a monolayer over a large area (up to several cm^2) at the water/hexane interface. Then the nanomembranes were transferred carefully from the "soft" air−water interface onto the ITO electrodes as depicted in our method reported elsewhere. (Wu et al., 2016) The disordered nanomembranes-based ECL electrode was prepared by a dropping method with the same amount of $Au@SiO_2$ NPs.

Preparation and modification of $Ru@SiO_2$ nanoparticles

Based on the previous studies (Dong et al., 2016; Zhang and Dong, 2006), $Ru@SiO_2$ nanoparticles were prepared as follows: First, 1.80 mL of Triton X-100 were mixed with 7.5 mL of cyclohexane, 340 μL of 40 mM $Ru(bpy)_3^{2+}$ and 1.8 mL of n-hexanol. After stirring for 30 min, 0.1 mL of TEOS was added into the solution. Then, the polymerization reaction was started by adding 60 μL of $NH_3 \cdot H_2O$. The solution was stirred for 24 h to obtain $Ru@SiO_2$ NPs, which were isolated by acetone, and followed by centrifuging and washing with isopropanol. The precipitation was dispersed with isopropanol to a final volume of 15 mL. In order to carboxylate the surface of $Ru@SiO_2$ NPs, 62 mg of 3-(Triethoxysilyl)propylsuccinic anhydride were added and heated at 85℃ for 24 h. Finally, the nanoparticles were centrifuged at 8000 rpm for three times and diluted with deionized water to 15 mL.

Modification of $Ru@SiO_2$ NPs with Ab_2.

1 mL of $Ru@SiO_2$ NPs were mixed with 400 μL EDC (0.35 M) and NHS (0.1 M) solution for 40 min under stirring. Subsequently, 200 μL of Ab_2 (0.1 mg/mL) were added and stirred for 12 h at room temperature. Finally, the mixture was centrifuged and washed two times with water. Then the mixture was blocked by BSA solution for 1 h at room temperature, and thereafter centrifuged at 8000 rpm for 15 min. The precipitation was dispersed into 2 mL of 0.01M PBS (pH 7.4).

Fabrication of the PSA ECL biosensor

Firstly, a MASNE was added into the mixture solution containing 400 μL of EDC (0.35 M) and NHS (0.1 M) for 40 min. Then, 10 μL of Ab_1 (0.1 mg/mL) were dropped

on the MASNE and incubated for 2 h at 25℃. Subsequently, the MASNE was washed with 0.01 M PBS (pH 7.4) to remove the nonspecific absorption of Ab_1. The MASNE was then blocked with 3% BSA blocking solution for 2 h to block non-specific binding sites and washed with the washing buffer thoroughly. Next, 10 μL of PSA was dropped on the MASNE-Ab_1 and incubated for 2 h at 25℃. Thereafter, the decorated MASNE was washed with 0.01 M PBS (pH 7.4). At last, the decorated MASNE was incubated in the Ru@SiO_2-Ab_2 NP solution for 4 h, and then washed with the washing buffer. The ECL tests were performed in 0.1 M PBS (pH=7.4) containing 0.1 mM TPrA and the linear scan potential was applied from 0-1.35 V with a scan rate of 100 mV/s.

SUPPLEMENTAL REFERENCES

Cheng, Z., Choi, N., Wang, R., Lee, S., Moon, K.C., Yoon, S.-Y., Chen, L., and Choo, J. (2017). Simultaneous detection of dual prostate specific antigens using surface-enhanced raman scattering-based immunoassay for accurate diagnosis of prostate cancer. ACS Nano *11*, 4926-4933.

Dong, Y.-P., Chen, G., Zhou, Y., and Zhu, J.-J. (2016). Electrochemiluminescent sensing for caspase-3 activity based on $Ru(bpy)_3^{2+}$-doped silica nanoprobe. Anal. Chem. *88*, 1922-1929.

Frens, G. (1973). Controlled nucleation for the regulation of the particle size in monodisperse gold suspensions. Nature *241*, 20-22.

Haiss, W., Thanh, N.T.K., Aveyard, J., and Fernig, D.G. (2007). Determination of size and concentration of gold nanoparticles from UV−Vis spectra. Anal. Chem. *79*, 4215-4221.

Li, J.F., Huang, Y.F., Ding, Y., Yang, Z.L., Li, S.B., Zhou, X.S., Fan, F.R., Zhang, W., Zhou, Z.Y., Wu de, Y., *et al.* (2010). Shell-isolated nanoparticle-enhanced Raman spectroscopy. Nature *464*, 392-395.

Nam, J.-M., Thaxton, C.S., and Mirkin, C.A. (2003). Nanoparticle-based bio-bar codes for the ultrasensitive detection of proteins. Science *301*, 1884-1886.

Qi, H., Li, M., Dong, M., Ruan, S., Gao, Q., and Zhang, C. (2014). Electrogenerated chemiluminescence peptide-based biosensor for the determination of prostate-specific antigen based on target-induced cleavage of peptide. Anal. Chem. *86*, 1372-1379.

Rissin, D.M., Kan, C.W., Campbell, T.G., Howes, S.C., Fournier, D.R., Song, L., Piech, T., Patel, P.P., Chang, L., Rivnak, A.J., *et al.* (2010). Single-molecule enzyme-linked immunosorbent assay detects serum proteins at subfemtomolar concentrations. Nat. Biotechnol. *28*, 595.

Shao, K., Wang, B., Nie, A., Ye, S., Ma, J., Li, Z., Lv, Z., and Han, H. (2018). Target-triggered signal-on ratiometric electrochemiluminescence sensing of PSA based on MOF/Au/G-quadruplex. Biosens. Bioelectron. *118*, 160-166.

Wu, H., Li, C., Zhao, Z., Li, H., and Jin, Y. (2016). Free-standing monolayered metallic nanoparticle networks as building blocks for plasmonic nanoelectronic junctions. ACS Appl. Mater. Interfaces *8*, 1594-1599.

Yu, X., Munge, B., Patel, V., Jensen, G., Bhirde, A., Gong, J.D., Kim, S.N., Gillespie, J., Gutkind,

J.S., Papadimitrakopoulos, F., *et al.* (2006). Carbon nanotube amplification strategies for highly sensitive immunodetection of cancer biomarkers. J. Am. Chem. Soc. *128*, 11199-11205.

Zhang, L., and Dong, S. (2006). Electrogenerated chemiluminescence sensors using $Ru(bpy)_3^{2+}$ doped in silica nanoparticles. Anal. Chem. *78*, 5119-5123.

Zheng, G., Patolsky, F., Cui, Y., Wang, W.U., and Lieber, C.M. (2005). Multiplexed electrical detection of cancer markers with nanowire sensor arrays. Nat. Biotechnol. *23*, 1294.